

Global heat uptake by inland waters

I. Vanderkelen¹, N. P. M. van Lipzig², D. M. Lawrence³, B. Droppers⁴, M. Golub⁵, S. N. Gosling⁶, A. B. G. Janssen⁴, R. Marcé^{7,8}, H. Müller Schmied^{9,10}, M. Perroud¹¹, D. Pierson⁵, Y. Pokhrel¹², Y. Satoh¹³, J. Schewe¹⁴, Sonia I. Seneviratne¹⁵, V. M. Stepanenko^{16,17}, R. I. Woolway¹⁸ and W. Thiery^{1,15}

¹Vrije Universiteit Brussel, Department of Hydrology and Hydraulic Engineering, Brussels, Belgium

²KU Leuven, Department of Earth and Environmental Sciences, Leuven, Belgium

³National Center for Atmospheric Research, Boulder, Colorado, USA

⁴Wageningen University & Research, Water Systems and Global Change group, Wageningen, The Netherlands

⁵Uppsala University, Department of Ecology and Genetics, Uppsala, Sweden

⁶University of Nottingham, School of Geography, Nottingham, United Kingdom

⁷Catalan Institute for Water Research, Girona, Spain

⁸University of Girona, Girona, Spain

⁹Goethe University Frankfurt, Institute of Physical Geography, Frankfurt am Main, Germany

¹⁰Senckenberg Leibniz Biodiversity and Climate Research Centre (SBIK-F), Frankfurt am Main, Germany

¹¹University of Geneva, Institute for Environmental Sciences, Geneva, Switzerland

¹²Michigan State University, Department of Civil and Environmental Engineering, East Lansing, MI, United States

¹³National Institute for Environmental Studies, Center for Global Environmental Research, Tsukuba, Japan

¹⁴Potsdam Institute for Climate Impact Research, Transformation Pathways, Potsdam, Germany

¹⁵ETH Zurich, Institute for Atmospheric and Climate Science, Zurich, Switzerland

¹⁶Moscow State University, Research Computing Center, Moscow, Russia

¹⁷Moscow State University, Faculty of Geography, Moscow, Russia

¹⁸Dundalk Institute of Technology, Centre for Freshwater and Environmental Studies, Dundalk, Ireland

Key Points:

- We use a unique combination of lake models, hydrological models, and Earth System models to quantify global heat uptake by inland waters.
- Heat uptake by inland waters over the industrial period amounts up to 2.8×10^{20} J, or 3.1% of the continental heat uptake.
- The thermal energy of the water trapped on land due to dam construction (27×10^{20} J) is ~ 9.6 times larger than inland water heat uptake.

Corresponding author: Inne Vanderkelen, inne.vanderkelen@vub.be

Abstract

Heat uptake is a key variable for understanding the Earth system response to greenhouse gas forcing. Despite the importance of this heat budget, heat uptake by inland waters has so far not been quantified. Here we use a unique combination of global-scale lake models, global hydrological models and Earth system models to quantify global heat uptake by natural lakes, reservoirs and rivers. The total net heat uptake by inland waters amounts to $2.8 \pm 4.3 \times 10^{20}$ J over the period 1900-2020, corresponding to 3.1% of the energy stored on land. The overall uptake is dominated by natural lakes (126%), followed by reservoir warming (2.6%). Rivers contribute negatively (-28.7%) due to a decreasing water volume. The heat of the water volume stored in reservoirs exceeds inland water heat uptake by a factor of ~ 9.6 . Our results underline the importance of inland waters for buffering atmospheric warming caused by enhanced greenhouse gas concentrations.

Plain Language Summary

Human-induced emissions of CO₂ and other greenhouse gases cause energy accumulation in the Earth system. Oceans trap most of this excess energy, thereby largely buffering the warming of the atmosphere. However, the fraction of excess energy stored in lakes, reservoirs and rivers is currently unknown, despite the high heat capacity of water. Here we quantify this human-induced heat storage, and show that it amounts up to 3.1% of the energy stored on land. The increase in heat storage from 1900 to 2020 is dominated by warming of lakes. The thermal heat contained in the water added on land due to dam construction is nearly ten times smaller. Our study overall highlights the importance of inland waters – next to oceans, ice and land – for buffering atmospheric warming, especially on regional scale.

1 Introduction

Increasing greenhouse gas concentrations in the atmosphere cause a net heat uptake in the Earth System. Over 90% of this extra thermal energy is stored in the oceans, causing ocean warming and global sea level rise through thermal expansion (Rhein et al., 2013). The most recent estimates of heat uptake are described in the Special Report on the Ocean and Cryosphere in a Changing Climate (SROCC) by the Intergovernmental Panel on Climate Change (IPCC). The report concludes that the ocean has taken up $4.35 \pm 0.8 \times 10^{21}$ J yr⁻¹ in the upper-700 m of water and $2.25 \pm 0.64 \times 10^{21}$ J yr⁻¹ between the depths of 700-2000 m, respectively (averages of 1998-2017 compared to 1971-1990), and attributes this increase to anthropogenic forcings (Bindoff et al., 2019). The remaining excess heat is taken up by melting sea and land ice, by specific heating and water evaporation in the atmosphere and by warming of the continents (Trenberth, 2009).

Despite the key role of heat uptake in driving Earth system response to greenhouse gas forcing, currently little is known about global-scale heat uptake by inland waters. Inland waters include natural lakes, man-made reservoirs, rivers and wetlands, with lakes covering 1.8% of the global land area (Messenger et al., 2016) and rivers 0.58% of the global non-glaciated land area (Allen & Pavelsky, 2018). However, the abundance and total area covered by inland waters (natural and/or artificial) is continuously changing (Pekel et al., 2016). For example, reservoir expansion following dam construction experienced a marked acceleration during the 1960s and 1970s, but levelled off after the 1980s, now covering 0.2% of the global land area (Lehner et al., 2011). Despite occupying <3% of the global land surface, inland waters play an important role in the climate system (e.g., Subin et al., 2012; Docquier et al., 2016; Vanderkelen et al., 2018a; Choulga et al., 2019) and are sentinels of climate change (e.g., Adrian et al., 2009; Schewe et al., 2014; O'Reilly et al., 2015; Woolway & Merchant, 2019). Compared to other types of land surfaces, water (i) has a higher specific heat capacity, (ii) typically has a lower albedo, (iii) allows

83 for radiation penetration below the surface, and (iv) seasonally mixes warmer surface
84 masses to deeper layers. Consequently, inland waters are generally regarded as heat reser-
85 voirs compared to adjacent land. In addition, lake surface temperatures have been ob-
86 served to have increased rapidly in recent decades, in some locations even faster than
87 ambient air temperatures (O’Reilly et al., 2015; Schneider & Hook, 2010). This is not
88 only the result of an increased lake heat uptake due to increasing air temperatures, but
89 can be attributed to an interplay between changes in ice cover duration and stratifica-
90 tion, solar radiation and lake characteristics (Austin & Allen, 2011; Shatwell et al., 2019).
91 Moreover, the warming rates are spatially very heterogeneous (O’Reilly et al., 2015).

92 To quantify the heat uptake by inland waters, an estimation of both the water vol-
93 umes and evolution of water temperature profiles is necessary. Water temperature ob-
94 servations of lakes, reservoirs, rivers and wetlands are however sparse and spatially lim-
95 ited. So far, studies of energy fluxes and heat storage have been limited to individual lakes
96 (Heiskanen et al., 2015; Nordbo et al., 2011; Strachan et al., 2016). To overcome this,
97 global models are developed for estimating water temperatures on local, regional and global
98 scales.

99 In this study, we develop the first estimate of the global-scale heat uptake by in-
100 land waters over the period 1900-2020. To this end, we combine global lake and hydro-
101 logical simulations from the Inter-Sectoral Model Intercomparison Project (ISIMIP) with
102 a river temperature parameterisation and spatially-explicit data sets of lake abundance,
103 reservoir area expansion and lake depth. This enables us to quantify the heat uptake by
104 natural lakes, reservoirs and rivers. We do not consider the contribution of wetlands and
105 floodplains, given their highly disperse spatial and temporal character and limited data
106 availability. Next, we also quantify the redistribution of heat from ocean to land due to
107 increased inland water storage as a result of the construction of reservoirs. By provid-
108 ing a first estimate of inland water heat uptake, this study provides new advances in the
109 quantification of the global heat budget.

110 2 Data and Methods

111 2.1 Lake and reservoir heat content

112 The ISIMIP initiative is a recent effort to provide consistent climate impact sim-
113 ulations across different sectors which allows for the integration and comparison of global
114 hydrological and lake model simulations (Frieler et al., 2017). For lake water tempera-
115 tures, we used the global ISIMIP2b simulations from two one-dimensional lake models:
116 the Community Land Model 4.5 (CLM4.5, Oleson et al., 2013) including the Lake, Ice,
117 Snow and Sediment Simulator (LISSS, Subin et al., 2012), and SIMSTRAT-UoG, a phys-
118 ically sophisticated k - ϵ model (Goudsmit et al., 2002, see table ?? for an overview). Fol-
119 lowing the ISIMIP2b protocol, simulations are performed at a 0.5° by 0.5° spatial res-
120 olution using bias-adjusted atmospheric forcing data from four Earth System Models (ESMs:
121 GFDL-ESM2M, HadGEM2-ES, IPSL-CM5A-LR and MIROC5). SIMSTRAT-UoG does
122 not represent human-influences, while CLM4.5 assumes that land use and human influ-
123 ences (irrigation extent, land use, population and GDP) are constant at the 2005 level.
124 We use ESM simulations for the historical period with historical climate and greenhouse
125 gas conditions, ranging from 1900 to 2005 and Representative Concentration Pathway
126 6.0 simulations for the period 2006-2020 (Frieler et al., 2017). The lake models simulate
127 a representative lake with a constant depth in each grid cell, of which the extent is given
128 by the lake area fraction of that grid cell. Using the four climate forcings for each lake
129 model results in a total of 8 simulations of spatially-explicit global-scale lake tempera-
130 tures.

131 Global lake area distribution is given by the HydroLAKES dataset (Messenger et
132 al., 2016), containing 1.42 million individual polygons of natural lakes. This data set is

133 linked to the Global Reservoir and Dam data set v. 1.3 (GRanD, Lehner et al., 2011)
 134 consisting of 7250 reservoir polygons (Lehner et al., 2011). We convert both HydroLAKES
 135 and GRanD polygons to lake area fraction on a 0.5° by 0.5° grid to match the ISIMIP
 136 resolution. Reservoir construction is provided by GRanD, and changes in reservoir area
 137 are accounted for by creating annual lake area fraction maps, in which reservoir areas
 138 are added in their year of construction. Natural lakes which become controlled by a dam
 139 are categorized as 'natural lakes' based on information from GRanD. As GRanD pro-
 140 vides construction years up to 2017, we assume a constant reservoir area from 2017 to
 141 2020. Lake and reservoir depths are obtained from the Global Lake Database v.3 (GLDB,
 142 Kourzeneva, 2010; Choulga et al., 2014, 2019), providing estimates of mean lake depth
 143 for every land grid cell. This data is remapped from its original $30''$ (~ 1 km grid) to
 144 the 0.5° by 0.5° resolution using bi-linear interpolation.

145 Annual lake heat content Q_{lake} [J], per grid cell is calculated as

$$Q_{lake} = c_{liq} A_{lake} \rho_{liq} \sum_{n=1}^{n=nlayers} T_n d_n$$

146 with c_{liq} ($J kg^{-1} K^{-1}$) the specific heat capacity of liquid water (here taken con-
 147 stant at $4188 J kg^{-1} K^{-1}$), A_{lake} (m^2) the lake area, ρ_{liq} ($kg m^{-3}$) the density of liq-
 148 uid water (here taken at $1000 kg m^{-3}$), and the sum of annual mean temperatures T_n
 149 (K) over all lake layers, where d_n (m) is the layer thickness. As the layering of each lake
 150 model is different (table ??), lake heat per layer is rescaled by calculating the weights
 151 of the model layer depths relative to the models' grid cell lake depth. These weights are
 152 then applied on the grid cell lake depth from GLDB. This allows for a consistent vol-
 153 ume computation. To also ensure a consistent lake coverage across the different lake mod-
 154 els, the water temperatures are spatially interpolated to the lake coverage map derived
 155 from HydroLAKES using nearest neighbour remapping. The Caspian Sea is included in
 156 the analysis, as this inland sea is often not accounted for in ocean heat content estimates
 157 (e.g. Cheng et al., 2017). We define the spatial extent of natural lakes by the lake ex-
 158 tent in 1900. Heat content anomalies, hereafter denoted as heat uptake, are computed
 159 relative to the average lake heat content in 1900-1929, hereafter referred to as pre-industrial
 160 period) and represent changes in lake and reservoir temperatures. Changes in the amount
 161 of water stored on land by the construction of reservoirs are also taken into account, thereby
 162 assuming the water temperature of the constructed reservoir is given by the grid cell lake
 163 temperature. We do not consider inter-annual variations in lake and reservoir volumes.
 164 Total annual global heat uptake is calculated by summing all grid cells.

165 2.2 River heat content

166 River water mass is retrieved from the grid-scale monthly river storage ($kg m^{-2}$)
 167 given by the two Global Hydrological Models from the ISIMIP 2b global water sector
 168 providing this variable: the Minimal Advanced Treatments of Surface Interaction and
 169 Runoff (MATSIRO, N. Y. Pokhrel et al., 2015) and WaterGAP2 (Müller Schmied et al.,
 170 2016, see table ??), by multiplying with the grid cell area and taking the annual mean.
 171 Annual grid cell river water temperatures are estimated using the global non-linear re-
 172 gression model of Punzet et al. (2012) with the global coefficients and an efficiency fit
 173 of 0.87. This regression prescribes river temperatures based on monthly gridded air tem-
 174 peratures, which are given by the four different ESM forcings (GFDL-ESM2M, HadGEM2-
 175 ES, IPSL-CM5A-LR and MIROC5). River heat content, Q_{river} [J], is calculated as

$$Q_{river} = c_{liq} m_{river} T_{river}$$

176 with m_{river} (kg) the water storage in the grid cell rivers and T_{river} (K) the river
 177 temperature. As for lakes, river heat uptake is defined as the anomaly compared to the

178 average river heat content in the reference period 1900-1929 and consists of the change
 179 in temperature and the change in water stored in the rivers. This approach uses a to-
 180 tal of 8 ISIMIP simulations to calculate river heat uptake. The set-up of the models, dic-
 181 tated by the ISIMIP protocol, allows the direct comparison of the resulting lake, reser-
 182 voir and river heat uptake.

183 **3 Inland water heat uptake**

184 Natural lakes have taken up $2.9 \pm 2.0 \times 10^{20}$ J (\pm one standard deviation of the 8
 185 simulations used) averaged over the period 2011-2020, relative to pre-industrial times
 186 (1900-1929; Table 1) due to an increase of lake water temperatures integrated over the
 187 lake column. Lake heat uptake increased continuously from the 1980s onwards, follow-
 188 ing the trend of increasing atmospheric temperatures (Figs. 1a, ??). In the last 30 years,
 189 the mean trend in global lake heat uptake of the model simulations is 8.1×10^{18} J year⁻¹.

190 The construction of dams and the resulting artificial reservoirs have increased global
 191 lake volume by 3.2% (Messenger et al., 2016, Fig. ??b). The steep increase in reservoir
 192 heat uptake from the 1980s onwards stems from the combination of accelerated reser-
 193 voir construction, making more water on land available for warming, and regional emer-
 194 gence of warming signals due to climate change during this period (Fig. 1b). In total,
 195 reservoirs have taken up $5.9 \pm 2.7 \times 10^{18}$ J on average in the period 2011-2020, compared
 196 to pre-industrial times (Table 1), which is about 2% of the total heat uptake by inland
 197 waters.

198 Global heat uptake by rivers encompasses large uncertainties and no detectable trend.
 199 In the late 1960s the ensemble mean heat uptake shifts to overall negative heat uptake
 200 values compared to pre-industrial values (Fig 1c). Global-scale stream temperatures show
 201 a clear positive trend, reflecting the increase in air temperatures (Fig. ??, a-d). How-
 202 ever, global-scale river storage is marked by large inter-annual variability for both global
 203 hydrological models (Fig. ??, e-l), thereby effectively masking the positive temperature
 204 trend in the resulting river heat uptake. River storage evolution is dictated mainly by
 205 the ESM forcing, as differences in river storage between the four different ESM forcings
 206 are more pronounced than between the two global hydrological models (Fig. ??). Both
 207 GFDL-ESM2M-driven river storage simulations have higher variability compared to the
 208 other simulations. Altogether, with a heat uptake of $-0.15 \pm 2.3 \times 10^{20}$ J averaged for
 209 2011 to 2020, compared to pre-industrial times, rivers contribute negatively to total heat
 210 uptake by inland waters, but their contribution is accompanied by a large variability, as
 211 well as uncertainty originating from the spread across climate forcings.

212 The total heat uptake in inland waters is thus dominated by the heat uptake of nat-
 213 ural lakes, accounting for 126% of the average total net increase by 2020, while reser-
 214 voir heating has taken up 2.6% and rivers contributed negatively with -28.7% in 2020,
 215 but the latter with a large uncertainty (Fig. 3a).

216 Most lake heat uptake is concentrated in the major lake regions of the world. The
 217 Laurentian Great Lakes, including Lakes Superior, Michigan, Huron, Erie and Ontario
 218 in central North America make up 12.40% of global lake volume (Messenger et al., 2016).
 219 These lakes all demonstrate a steady increase in heat uptake from the 1980s onwards (Fig.
 220 2b), resulting in a total uptake of $1.45 \pm 0.74 \times 10^{19}$ J (5.2% of global inland water heat
 221 uptake) compared to pre-industrial times with a trend of 4.2×10^{17} J year⁻¹ over the last
 222 30 years. The spatial pattern of heat uptake is mainly dictated by the bathymetry and
 223 resulting lake volume: the deeper Lake Michigan and Lake Superior have taken up more
 224 heat compared to the other lakes, while the much shallower Lake Erie has the lowest heat
 225 uptake estimates (Fig. 2a). The warming of these seasonally-ice covered lakes, and their
 226 impact on the surrounding weather and climate has been extensively studied (e.g. Zhong
 227 et al., 2019; Gronewold et al., 2015; Austin & Allen, 2011) and recently, O'Reilly et al.

228 (2015) reported that their surface is warming faster than most other major lakes world-
 229 wide.

230 The African Great Lakes region in East Africa, consisting of Lake Victoria, Tan-
 231 ganyika, Kivu, Kyoga, Albert and Edward (12.38% of global lake volume Messenger et
 232 al. (2016)), are known to affect the local weather and climate conditions (Thiery et al.,
 233 2014, 2015, 2016, 2017; Vanderkelen et al., 2018b; Van de Walle et al., 2019) and their
 234 water temperatures are observed to be warming (Katsev et al., 2014; O'Reilly et al., 2003;
 235 Tierney et al., 2010). We find that the heat uptake is largest in Tanganyika, the lake with
 236 the highest volume in the region (Fig. 2c). Overall, the African Great Lakes show an in-
 237 crease in heat over the whole study period, of the same order of magnitude as the Lau-
 238 rentian Great Lakes (Fig. 2d, a total heat uptake of $4.23 \pm 1.48 \times 10^{19}$ J, 15.1% of global
 239 inland water heat uptake). The Great European lakes, including Lake Ladoga and Onega,
 240 the largest lakes in Europe, show a smaller increase compared to other major lake re-
 241 gions, corresponding to the smaller volume of the lakes, but the lake heat content shows
 242 a sudden increase from the 1990s (Fig. 2e,f; total heat uptake of $2.20 \pm 0.91 \times 10^{18}$ J, 0.79%
 243 of global inland water heat uptake). The Amazon, world's highest discharge river, de-
 244 picts no temporal trend in river heat uptake, but the uncertainty is large, mainly ow-
 245 ing to the diverging river mass estimations (Fig. 2h; heat uptake of $0.18 \pm 2.50 \times 10^{20}$ J,
 246 6.4% of global inland water heat uptake). Heat uptake increases towards the river mouth,
 247 as the water volume increases (Fig. 2g). To summarize, the global picture of positive lake
 248 heat uptake is confirmed at the regional scale by all model combinations. At the river
 249 basin scale, however, the uncertainties of river heat uptake are large and there is no agreed
 250 signal, in line with global estimates.

251 4 Heat redistribution due to reservoir area expansion

252 In the second half of the 20th century, reservoir capacity strongly increased, rais-
 253 ing the water volume stored on land and offsetting sea level rise by 30 mm (Chao et al.,
 254 2008; Lehner et al., 2011, Fig. ??b). This extra water stored on land does not only in-
 255 crease the potential for taking up excess atmospheric heat (Sect. 2), but also carries en-
 256 ergy in itself. By constructing reservoirs, humans are thus not only redistributing mass
 257 from the oceans to the land, but also the thermal energy carried within this water. This
 258 heat redistribution by reservoir expansion is growing over time, following the increas-
 259 ing number of reservoirs constructed (Fig. 3b). During the historical period, $27 \pm 2.1 \times 10^{20}$
 260 J of heat was redistributed from ocean to land, exceeding inland water heat uptake from
 261 climate change by a factor of ~ 9.6 .

262 5 Discussion and conclusions

263 Large lakes take up most heat, as they have the largest volume to warm up. The
 264 increase in lake heat content complies with recent observations of increasing lake sur-
 265 face temperatures and reported changes in mixing regimes (O'Reilly et al., 2015; Wool-
 266 way & Merchant, 2019) and is robust for different lake regions. For lakes that are sea-
 267 sonally ice-covered, lake heat uptake mainly occurs during the open water season (Mishra
 268 et al., 2011). Therefore, an earlier ice break up and later ice formation could possibly
 269 explain the sudden rise in lake heat in the Great European Lakes. The difference between
 270 the two lake models (Fig. ??) could arise from differences in the structure of the mod-
 271 els, like lake layers and internal physics.

272 River heat uptake is negative in most simulations during the second half of the 20th
 273 century. This seemingly contradictory result stems from a decrease in river storage, which
 274 could be attributed to less precipitation or the construction of reservoirs, lowering wa-
 275 ter flow in rivers or to drying of rivers by increased land evaporation due to global warm-
 276 ing or increased water use. These changes in river storage should, however, be taken with
 277 care, as the uncertainties are very large. In addition, no conclusions can be made about

278 global trends in observed streamflow, because changes in streamflow and the hydrologi-
279 cal conditions causing it, are characterized by complex spatial patterns (Gudmundsson
280 et al., 2019; Müller Schmied et al., 2016).

281 The quantification of heat uptake facilitates comparison of the effects of climate
282 change on different components of the climate system. Globally, inland waters have taken
283 up $\sim 0.08\%$ of heat compared to oceans. The continental heat uptake occurs through a
284 heat flux into the solid surface of the lithosphere and has been estimated between 9.1
285 and 10.4×10^{21} J (Beltrami, 2002; Huang, 2006) for the period 1950-2000 based on bore-
286 hole temperature observations. Estimates based on the Coupled Model Intercompari-
287 son Project Phase 5 (CMIP5) are consistently lower ($1 \pm 5 \times 10^{21}$ J), mainly due to the
288 limited depth of the bottom boundary of the land surface schemes of the Earth system
289 models (Cuesta-Valero et al., 2016). Relative to the geophysical estimate reported by
290 Beltrami (2002), the share of inland waters is $\sim 3.1\%$, while inland waters cover about
291 $\sim 2.58\%$ of the global continental area. This comparison has to be taken with care, as
292 the borehole-based estimations of heat uptake are only quantified until 2000 and surface
293 air temperatures have risen at record rates since then (Rhein et al., 2013).

294 The redistribution of heat by reservoir construction, is equivalent to $\sim 38\%$ of the
295 land mass heat uptake. It increases the potential of storing extra heat on land by warm-
296 ing the water of the created reservoirs. In particular, this might cause local impacts such
297 as masking surface temperature increase over the historical period by their buffering ca-
298 pacity. In addition, the extra continental water storage by reservoir expansion could have
299 a dampening effect on local temperature extremes and could affect river temperatures
300 downstream. Furthermore, reservoirs could cause alterations in extreme precipitation (Degu
301 et al., 2011), but the physical mechanisms behind this are not yet well understood. It
302 is therefore important to account for reservoir expansion and resulting heat redistribu-
303 tion in Earth System Models, to increase our understanding of how reservoirs affect the
304 climate (Y. N. Pokhrel et al., 2016; Nazemi & Wheeler, 2015; Wada et al., 2017). Cap-
305 turing heat redistribution by reservoir expansion could also increase the quality of cli-
306 mate change projections on regional to global scales.

307 Furthermore, lakes and rivers do not only have the potential for storing heat com-
308 ing from warming by excess greenhouse gases, but they also play a role in engineered heat
309 storage. Locally, lakes may serve as a source or sink for anthropogenic heat, for instance
310 as thermal heat pumps or cooling systems (Fink et al., 2014), while rivers have been used
311 by industries for their cooling water discharge potential (van Vliet et al., 2016).

312 There are several opportunities to refine the heat uptake calculations presented in
313 this study. First, the volume calculation does not account for lake hypsometry. By us-
314 ing average lake depths to multiply with lake area, the resulting total lake volumes are
315 reasonable, as most lakes have a linear hypsometric relationship (Busker et al., 2019; Mes-
316 sager et al., 2016; Choulga et al., 2014). This rectangular hypsometry assumption results
317 in relatively higher weights for the deeper lake layers, which makes our heat uptake es-
318 timates more conservative. Second, apart from reservoir construction, the heat calcu-
319 lation does not account for variations in lake and reservoir volumes, while changes in river
320 storage are included. This could have important effects, especially for lakes with a high
321 inter-annual variability. Recent advancements in remote sensing allow mapping global
322 surface water and its temporal variations (e.g. the Global Surface Water data set; Pekel
323 et al., 2016), but these assessments are time-limited to the satellite era. Third, as reser-
324 voir operation are modelled in the same way as natural lakes, the deep withdrawals related to reser-
325 voir operation are not considered. Deep withdrawals imply higher temperatures than sim-
326 ulated in natural lakes (Moreno-Ostos et al., 2008), leading to a potential underestima-
327 tion of the heat uptake by reservoirs. Furthermore, variations in heat capacity are not
328 considered in our analysis, which could lead to a lower estimate of heat uptake as the
329 specific capacity of ice is lower than that of water ($2117 \text{ J kg}^{-1} \text{ K}^{-1}$ compared to 4188
330 $\text{ J kg}^{-1} \text{ K}^{-1}$, respectively). In addition, the formation and melting of lake ice also re-

Table 1. Total heat uptake and trend for the different inland water components. Heat uptake is calculated as the average uptake during 2011-2020 relative to the reference period 1900-1929. Uncertainties are given by the ensemble standard deviation of the used simulations. Trends are calculated using a linear regression over the 30-year period 1991-2020.

	Heat uptake	Trend (1991-2020)
Natural lakes	$2.9 \pm 2.0 \times 10^{20}$ J	9.4×10^{18} J yr ⁻¹
Reservoirs	$0.059 \pm 0.027 \times 10^{20}$ J	0.19×10^{18} J yr ⁻¹
Rivers	$-0.15 \pm 2.3 \times 10^{20}$ J	2.7×10^{18} J yr ⁻¹
Uptake by climate change	$2.8 \pm 4.3 \times 10^{20}$ J	12.4×10^{18} J yr ⁻¹
Redistribution by reservoir expansion	$27 \pm 2.1 \times 10^{20}$ J	11.0×10^{18} J yr ⁻¹

331 lease and require heat, respectively. Phase changes are not considered explicitly, but they
 332 are included in the physics of the lake models and therefore in the simulated tempera-
 333 ture profiles. Next, variations in salinity of inland waters are not included. Salty water
 334 has a lower specific heat capacity than freshwater ($3986 \text{ J kg}^{-1} \text{ K}^{-1}$ for a salinity of sea
 335 water (3.5%) compared to $4188 \text{ J kg}^{-1} \text{ K}^{-1}$, (Brewer & Peltzer, 2019)), but applying
 336 this difference falls within the uncertainty range. Furthermore, by using global lake and
 337 hydrological models driven by ESM forcings, an extra uncertainty related to climate sen-
 338 sitivity is added to the calculations. Despite these limitations, this study is the first step
 339 towards estimating heat uptake by inland waters.

340 In this study, we show that inland water heat uptake during the historical period
 341 is substantial compared to continental heat uptake, calling for inclusion of this effect in
 342 global-scale assessments of heat uptake within the Earth system. Furthermore, we high-
 343 light that by constructing reservoirs, humans have redistributed heat from the ocean to
 344 land as well as increased the potential of storing more heat on land, given the higher heat
 345 capacity of water compared to land. Compared to the other components of the Earth
 346 system, this is a small term, but locally the impacts might be large. Our results over-
 347 all underline the potential importance of inland waters for buffering atmospheric warm-
 348 ing through enhanced anthropogenic greenhouse gas concentrations.

349 Acknowledgments

350 All ISIMIP2b simulations used for this assessment are publicly available through the Earth
 351 System grid Federation (ESGF, <https://esgf-data.dkrz.de/>). The HydroLAKES data
 352 is available at <https://www.hydrosheds.org/page/hydrolakes>, the GRanD data at
 353 <http://globaldamwatch.org/>, and the GLDB data at <http://www.lakemodel.net/>.
 354 The scripts used in the analysis are available on github: [https://github.com/VUB-HYDR/](https://github.com/VUB-HYDR/2020_Vanderkelen_etal_GRL)
 355 [2020_Vanderkelen_etal_GRL](https://github.com/VUB-HYDR/2020_Vanderkelen_etal_GRL). Inne Vanderkelen is a research fellow at the Research Foun-
 356 dation Flanders (FWO) (FWOTM920). Wim Thiery acknowledges the Uniscentia Foun-
 357 dation and the ETH Zurich Foundation for their support to this research. We are grate-
 358 ful to the Potsdam Institute for Climate Impact Research (PIK) for initiating and co-
 359 ordinating the ISIMIP initiative, and to the modelling centres for making their impact
 360 simulations publicly available through ESGF. Computational resources and services were
 361 provided by the Shared ICT Services Centre funded by the Vrije Universiteit Brussel,
 362 the Flemish Supercomputer Center (VSC) and FWO.

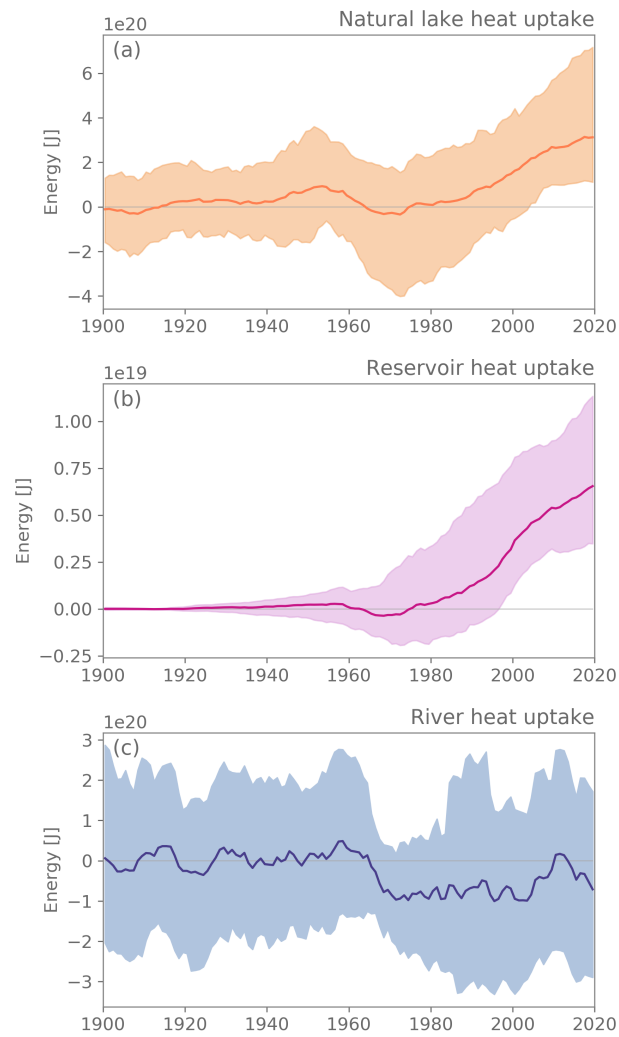


Figure 1. Heat uptake by natural lakes (a), reservoirs (b) and rivers (c). Shown are 10-year moving means relative to the 1900-1929 reference period. Note the different y-axis scales. Color shades represent uncertainty range shown as the standard deviation of the used simulations.

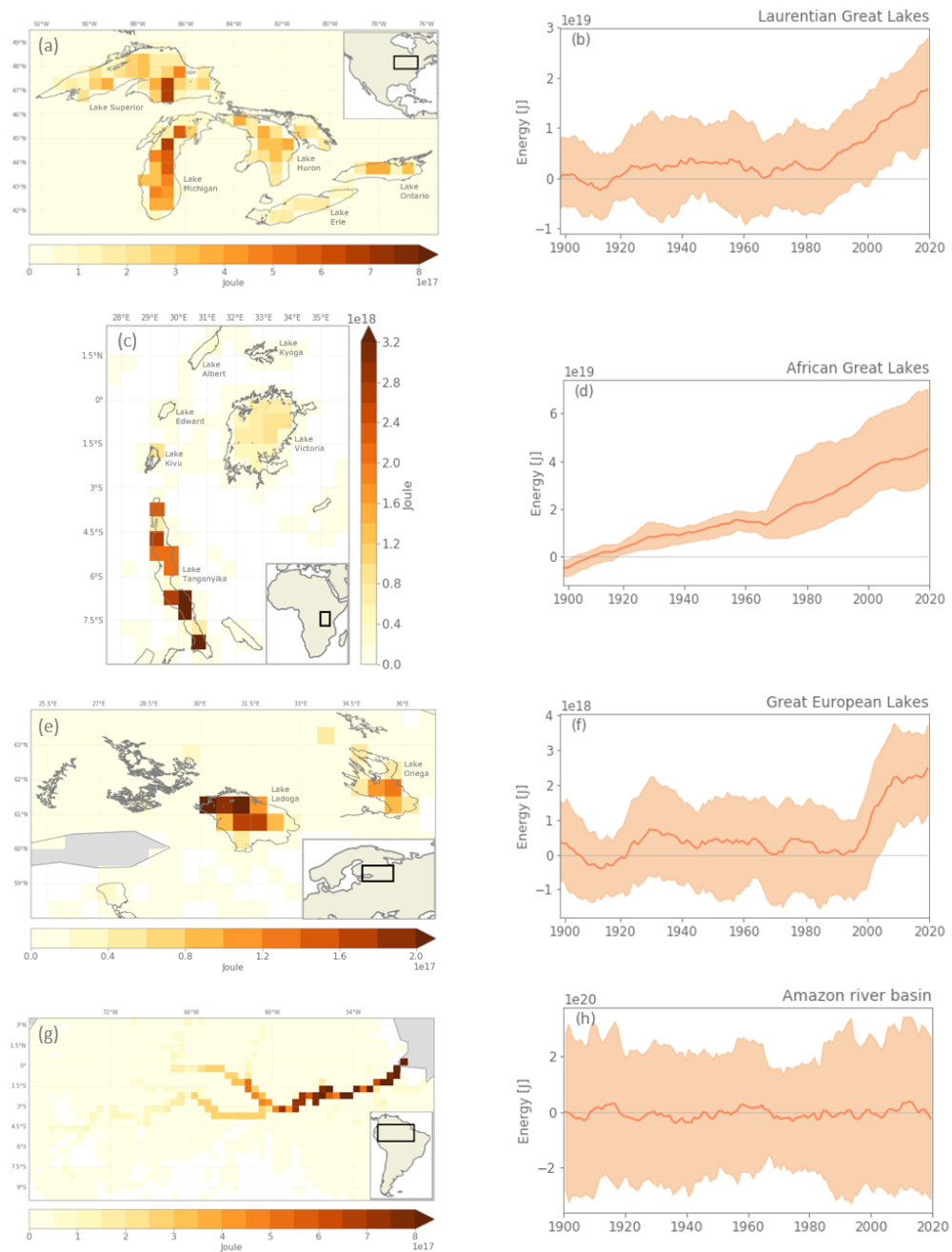


Figure 2. Heat uptake by the Laurentian Great lakes (a-b), the African Great Lakes (c-d), the Great European Lakes (e-f), and the Amazon River (g-h). The maps (a, c, e and g) represent the average heat uptake during the 2001-2020 period with the grey colors indicating ocean grid cells, and white colors grid cells without water. The graphs (b, d, f and h) show 10-year moving means, where the color shades represent uncertainty range shown as the standard deviation of the used simulations. The reference period is 1900-1929. Note the different y-axis scales.

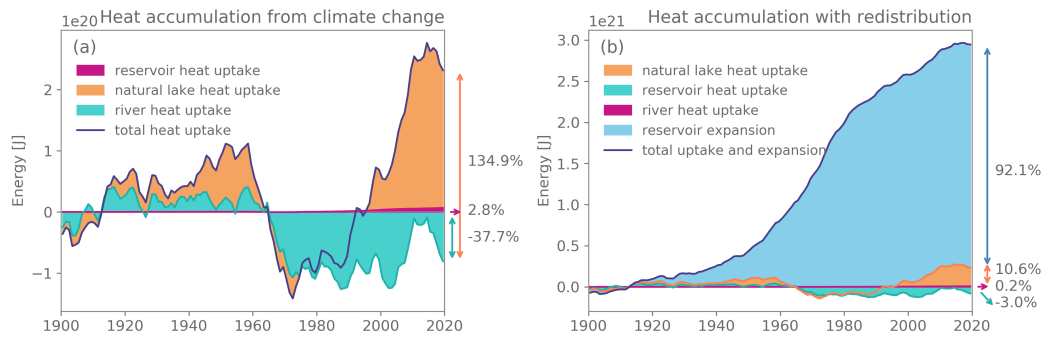


Figure 3. Inland water heat accumulation from climate change (a) and including redistribution by reservoir construction (b). Shown are 10-year moving ensemble means relative to the 1900-1929 reference period. Note the different y-axis scales.

References

- Adrian, R., O'reilly, C. M., Zagarese, H., Baines, S. B., Hessen, D. O., Keller, W.,
 ... Muir, J. (2009). Lakes as sentinels of climate change. *Limnology and
 Oceanography*, *54*(6), 2283–2297.
- Allen, G. H., & Pavelsky, T. (2018). Global extent of rivers and streams. *Science*,
361(6402), 585–588. doi: 10.1126/science.aat063
- Austin, J. A., & Allen, J. (2011). Sensitivity of summer Lake Superior thermal
 structure to meteorological forcing. *Limnology and Oceanography*, *56*(3), 1141–
 1154. doi: 10.4319/lo.2011.56.3.1141
- Beltrami, H. (2002). Earth's Long-Term Memory. *Perspectives: Paleoclimae*, *297*.
 doi: 10.1029/2001gl014310
- Bindoff, N. L., L Cheung, W. W., Kairo, J. G., Aristegui, J., Guinder, V. A., Hall-
 berg, R., ... Allison, E. (2019). Changing Ocean, Marine Ecosystems, and
 Dependent Communities. In *Ipc special report on the ocean and crosphere in a
 changing climate*.
- Brewer, P. G., & Peltzer, E. T. (2019). The Molecular Basis for the Heat Capac-
 ity and Thermal Expansion of Natural Waters. *Geophysical Research Letters*,
46(22), 13227–13233. doi: 10.1029/2019GL085117
- Busker, T., De Roo, A., Gelati, E., Schwatke, C., Adamovic, M., Bisselink, B., ...
 Cottam, A. (2019). A global lake and reservoir volume analysis using a surface
 water dataset and satellite altimetry. *Hydrology and Earth System Sciences*,
23(2), 669–690. doi: 10.5194/hess-23-669-2019
- Chao, B. F., Wu, Y. H., & Li, Y. S. (2008). Impact of artificial reservoir water im-
 poundment on global sea level. *Science*, *320*(5873), 212–214. doi: 10.1126/
 science.1154580
- Cheng, L., Trenberth, K. E., Fasullo, J., Boyer, T., Abraham, J., & Zhu, J. (2017).
 Improved estimates of ocean heat content from 1960 to 2015. *Science Ad-
 vances*, *3*(3), 1–10. doi: 10.1126/sciadv.1601545
- Choulga, M., Kourzeneva, E., Balsamo, G., Boussetta, S., & Wedi, N. (2019). Up-
 graded global mapping information for earth system modelling: An application
 to surface water depth at the ECMWF. *Hydrology and Earth System Sciences*,
23(10), 4051–4076. doi: 10.5194/hess-23-4051-2019
- Choulga, M., Kourzeneva, E., Zakharova, E., & Doganovsky, A. (2014). Estimation
 of the mean depth of boreal lakes for use in numerical weather prediction and
 climate modelling. *Tellus, Series A: Dynamic Meteorology and Oceanography*,
66(1). doi: 10.3402/tellusa.v66.21295
- Cuesta-Valero, F. J., García-García, A., Beltrami, H., & Smerdon, J. E. (2016).
 First assessment of continental energy storage in CMIP5 simulations. *Geophys-
 ical Research Letters*, *43*(10), 5326–5335. doi: 10.1002/2016GL068496
- Degu, A. M., Hossain, F., Niyogi, D., Pielke, R., Shepherd, J. M., Voisin, N., &
 Chronis, T. (2011). The influence of large dams on surrounding climate
 and precipitation patterns. *Geophysical Research Letters*, *38*(4), 1–7. doi:
 10.1029/2010GL046482
- Docquier, D., Thiery, W., Lhermitte, S., & van Lipzig, N. (2016). Multi-year wind
 dynamics around Lake Tanganyika. *Climate Dynamics*, *47*(9-10), 3191–3202.
 doi: 10.1007/s00382-016-3020-z
- Fink, G., Schmid, M., Wahl, B., Wolf, T., & Wüest, A. (2014). Heat flux modifi-
 cations related to climate-induced warming of large European lakes. *Water Re-
 sources Research*, *50*(3), 2072–2085. doi: 10.1002/2013WR014448
- Frieler, K., Lange, S., Piontek, F., Reyser, C. P. O., Schewe, J., Warszawski, L., ...
 Yamagata, Y. (2017). Assessing the impacts of 1.5 C global warming - sim-
 ulation protocol of the Inter-Sectoral Impact Model Intercomparison Project
 (ISIMIP2b). *Geoscientific Model Development*, *10*(12), 4321–4345. doi:
 10.5194/gmd-10-4321-2017

- 417 Goudsmit, G. H., Burchard, H., Peeters, F., & Wüest, A. (2002). Application of $k-\epsilon$
 418 turbulence models to enclosed basins: The role of internal seiches. *Journal of*
 419 *Geophysical Research C: Oceans*, *107*(12), 23–1. doi: 10.1029/2001jc000954
- 420 Gronewold, A. D., Anderson, E. J., Lofgren, B., Blanken, P. D., Wang, J., Smith,
 421 J., ... Bratton, J. (2015). Impacts of extreme 2013-2014 winter conditions
 422 on Lake Michigan’s fall heat content, surface temperature, and evaporation.
 423 *Geophysical Research Letters*, *42*(9), 3364–3370. doi: 10.1002/2015GL063799
- 424 Gudmundsson, L., Leonard, M., Do, H. X., Westra, S., & Seneviratne, S. I. (2019).
 425 Observed Trends in Global Indicators of Mean and Extreme Streamflow. *Geo-*
 426 *physical Research Letters*, *46*(2), 756–766. doi: 10.1029/2018GL079725
- 427 Heiskanen, J. J., Mammarella, I., Ojala, A., Stepanenko, V., Erkkilä, K. M., Miettinen,
 428 H., ... Nordbo, A. (2015). Effects of water clarity on lake stratification
 429 and lake-atmosphere heat exchange. *Journal of Geophysical Research*, *120*(15),
 430 7412–7428. doi: 10.1002/2014JD022938
- 431 Huang, S. (2006). 1851-2004 annual heat budget of the continental landmasses. *Geo-*
 432 *physical Research Letters*, *33*(4). doi: 10.1029/2005GL025300
- 433 Katsev, S., Aaberg, A. A., Crowe, S. A., & Hecky, R. E. (2014, oct). Recent warm-
 434 ing of lake kivu. *PLoS ONE*, *9*(10). doi: 10.1371/journal.pone.0109084
- 435 Kourzeneva, E. (2010). External data for lake parameterization in numerical weather
 436 prediction and climate modeling. *Boreal Environment Research*, *15*(2), 165–
 437 177. doi: 10.3402/tellusa.v64i0.15640
- 438 Lehner, B., Liermann, C. R., Revenga, C., Vörösmarty, C., Fekete, B., Crouzet,
 439 P., ... Wissler, D. (2011). High-resolution mapping of the world’s reservoirs
 440 and dams for sustainable river-flow management. *Frontiers in Ecology and the*
 441 *Environment*, *9*(9), 494–502. doi: 10.1890/100125
- 442 Messenger, M. L., Lehner, B., Grill, G., Nedeva, I., & Schmitt, O. (2016). Estim-
 443 ating the volume and age of water stored in global lakes using a geo-statistical
 444 approach. *Nature Communications*, *7*. doi: 10.1038/ncomms13603
- 445 Mishra, V., Cherkauer, K. A., & Bowling, L. C. (2011). Changing thermal dynam-
 446 ics of lakes in the Great Lakes region: Role of ice cover feedbacks. *Global and*
 447 *Planetary Change*. doi: 10.1016/j.gloplacha.2010.11.003
- 448 Moreno-Ostos, E., Marcé, R., Ordóñez, J., Dolz, J., & Armengol, J. (2008). Hy-
 449 draulic management drives heat budgets and temperature trends in a Mediter-
 450 ranean reservoir. *International Review of Hydrobiology*, *93*(2), 131–147. doi:
 451 10.1002/iroh.200710965
- 452 Müller Schmied, H., Adam, L., Eisner, S., Fink, G., Florke, M., Kim, H., ... Doll,
 453 P. (2016). Variations of global and continental water balance components as
 454 impacted by climate forcing uncertainty and human water use. *Hydrology and*
 455 *Earth System Sciences*, *20*(7), 2877–2898. doi: 10.5194/hess-20-2877-2016
- 456 Nazemi, A., & Wheeler, H. S. (2015). On inclusion of water resource management
 457 in Earth system models-Part 2: Representation of water supply and allocation
 458 and opportunities for improved modeling. *Hydrol. Earth Syst. Sci*, *19*, 63–90.
 459 doi: 10.5194/hess-19-63-2015
- 460 Nordbo, A., Launiainen, S., Mammarella, I., Leppäranta, M., Huotari, J., Ojala,
 461 A., & Vesala, T. (2011). Long-term energy flux measurements and energy
 462 balance over a small boreal lake using eddy covariance technique. *Journal of*
 463 *Geophysical Research Atmospheres*, *116*(2). doi: 10.1029/2010JD014542
- 464 Oleson, K. W., Lead, D. M. L., Bonan, G. B., Drewniak, B., Huang, M., Koven,
 465 C. D., ... Yang, Z.-L. (2013). *Technical Description of version 4.5 of the*
 466 *Community Land Model (CLM) Coordinating Lead Authors* (Tech. Rep.).
 467 NCAR/TN-503+STR. doi: 10.5065/D6RR1W7M
- 468 O’Reilly, C. M., Alin, S. R., Piisnier, P. D., Cohen, A. S., & McKee, B. A. (2003).
 469 Climate change decreases aquatic ecosystem productivity of Lake Tanganyika,
 470 Africa. *Nature*, *424*(6950), 766–768. doi: 10.1038/nature01833
- 471 O’Reilly, C. M., Sharma, S., Gray, D. K., Hampton, S. E., Read, J. S., Rowley,

- 472 R. J., ... Zhang, G. (2015). Rapid and highly variable warming of lake surface
473 waters around the globe. *Geophysical Research Letters*, *42*(24), 10773–10781.
474 doi: 10.1002/2015GL066235
- 475 Pekel, J. F., Cottam, A., Gorelick, N., & Belward, A. S. (2016, dec). High-resolution
476 mapping of global surface water and its long-term changes. *Nature*, *540*(7633),
477 418–422. doi: 10.1038/nature20584
- 478 Pokhrel, N. Y., Koirala, S., Yeh, P. J.-F., Hanasaki, N., Longuevvergne, L., Kanae,
479 S., & Oki, T. (2015). Incorporation of groundwater pumping in a global Land
480 Surface Model with the representation of human impacts. *Water Resources*
481 *Research*, *51*, 78–96. doi: 10.1002/2014WR015602
- 482 Pokhrel, Y. N., Hanasaki, N., Wada, Y., & Kim, H. (2016). Recent progresses in
483 incorporating human land-water management into global land surface models
484 toward their integration into Earth system models. *Wiley Interdisciplinary*
485 *Reviews: Water*, *3*(4), 548–574. doi: 10.1002/wat2.1150
- 486 Punzet, M., Voß, F., Voß, A., Kynast, E., & Bärlund, I. (2012). A global approach
487 to assess the potential impact of climate change on stream water temperatures
488 and related in-stream first-order decay rates. *Journal of Hydrometeorology*,
489 *13*(3), 1052–1065. doi: 10.1175/JHM-D-11-0138.1
- 490 Rhein, M., Rintoul, S. R., Aoki, S., Campos, E., Chambers, D., Feely, R. A., ...
491 Wang, F. (2013). Observations: Ocean. In *Climate change 2013 - the physical*
492 *science basis. contribution of working group i to the fifth assessment report*
493 *of the intergovernmental panel on climate change [stocker, t.f., d. Qin, g.-k.*
494 *plattner, m. tignor, s.k. allen, j. boschung, a. nauels, y. xia* (pp. 465–570).
495 Cambridge, United Kingdom and New York, NY, USA: Cambridge University
496 Press. doi: 10.1017/CBO9781107415324.015
- 497 Schewe, J., Heinke, J., Gerten, D., Haddeland, I., Arnell, N. W., Clark, D. B., ...
498 Kabat, P. (2014). Multimodel assessment of water scarcity under climate
499 change. *Proceedings of the National Academy of Sciences of the United States*
500 *of America*, *111*(9), 3245–3250. doi: 10.1073/pnas.1222460110
- 501 Schneider, P., & Hook, S. J. (2010). Space observations of inland water bodies show
502 rapid surface warming since 1985. *Geophysical Research Letters*, *37*(22). doi:
503 10.1029/2010GL045059
- 504 Shatwell, T., Thiery, W., & Kirillin, G. (2019, mar). Future projections of tem-
505 perature and mixing regime of European temperate lakes. *Hydrology and Earth*
506 *System Sciences*, *23*(3), 1533–1551. doi: 10.5194/hess-23-1533-2019
- 507 Strachan, I. B., Tremblay, A., Pelletier, L., Tardif, S., Turpin, C., & Nugent,
508 K. A. (2016). Does the creation of a boreal hydroelectric reservoir result
509 in a net change in evaporation? *Journal of Hydrology*, *540*, 886–899. doi:
510 10.1016/j.jhydrol.2016.06.067
- 511 Subin, Z. M., Riley, W. J., & Mironov, D. (2012). An improved lake model for
512 climate simulations: Model structure, evaluation, and sensitivity analyses in
513 CESM1. *Journal of Advances in Modeling Earth Systems*, *4*(2), 1–27. doi:
514 10.1029/2011MS000072
- 515 Thiery, W., Davin, E. L., Lawrence, D. M., Hirsch, A. L., Hauser, M., & Seneviratne,
516 S. I. (2017). Present-day irrigation mitigates heat extremes. *Journal of*
517 *Geophysical Research*, *122*(3), 1403–1422. doi: 10.1002/2016JD025740
- 518 Thiery, W., Davin, E. L., Panitz, H.-J., Demuzere, M., Lhermitte, S., & van Lipzig,
519 N. (2015). The Impact of the African Great Lakes on the Regional Climate.
520 *Journal of Climate*, *28*(10), 4061–4085. doi: 10.1175/JCLI-D-14-00565.1
- 521 Thiery, W., Davin, E. L., Seneviratne, S. I., Bedka, K., Lhermitte, S., & Van Lipzig,
522 N. P. (2016). Hazardous thunderstorm intensification over Lake Victoria.
523 *Nature Communications*, *7*. doi: 10.1038/ncomms12786
- 524 Thiery, W., Stepanenko, V. M., Fang, X., Jöhnk, K. D., Zhongshun, L., Martynov,
525 A., ... Van Lipzig, N. P. M. (2014). LakeMIP Kivu: evaluating the represen-
526 tation of a large, deep tropical lake by a set of one-dimensional lake models.

- 527 *Tellus A*, 66, 21390. doi: 10.3402/tellusa.v66.21390
- 528 Tierney, J. E., Russell, J. M., & Huang, Y. (2010). A molecular perspective on
529 Late Quaternary climate and vegetation change in the Lake Tanganyika
530 basin, East Africa. *Quaternary Science Reviews*, 29(5-6), 787–800. doi:
531 10.1016/j.quascirev.2009.11.030
- 532 Trenberth, K. E. (2009). An imperative for climate change planning: tracking
533 Earth’s global energy. *Current Opinion in Environmental Sustainability*, 1(1),
534 19–27. doi: 10.1016/j.cosust.2009.06.001
- 535 Van de Walle, J., Thiery, W., Brousse, O., Souverijns, N., Demuzere, M., & van
536 Lipzig, N. P. M. (2019). A convection-permitting model for the Lake Victoria
537 Basin: Evaluation and insight into the mesoscale versus synoptic atmospheric
538 dynamics. *Climate Dynamics*, 1, 3. doi: 10.1007/s00382-019-05088-2
- 539 Vanderkelen, I., van Lipzig, N. P. M., & Thiery, W. (2018a). Modelling the water
540 balance of Lake Victoria (East Africa)-Part 1: Observational analysis. *Hydrology and Earth System Sciences*, 22(10), 5509–5525. doi: 10.5194/hess-22-5509-
541 -2018
- 542 Vanderkelen, I., van Lipzig, N. P. M., & Thiery, W. (2018b). Modelling the wa-
543 ter balance of Lake Victoria (East Africa) - Part 2: Future projections. *Hydrology and Earth System Sciences*, 22(10), 5527–5549. doi: 10.5194/hess-22-5527-
544 -2018
- 545 van Vliet, M. T., van Beek, L. P., Eisner, S., Flörke, M., Wada, Y., & Bierkens,
546 M. F. (2016). Multi-model assessment of global hydropower and cooling water
547 discharge potential under climate change. *Global Environmental Change*. doi:
548 10.1016/j.gloenvcha.2016.07.007
- 549 Wada, Y., Bierkens, M. F. P., De Roo, A., Dirmeyer, P. A., Famiglietti, J. S.,
550 Hanasaki, N., ... Schmied, H. M. (2017). Human–water interface in hy-
551 drological modelling: current status and future directions. *Hydrol. Earth Syst.*
552 *Sci*, 21, 4169–4193. doi: 10.5194/hess-21-4169-2017
- 553 Woolway, R. I., & Merchant, C. J. (2019). Worldwide alteration of lake mixing
554 regimes in response to climate change. *Nature Geoscience*, 12(4), 271–276. doi:
555 10.1038/s41561-019-0322-x
- 556 Zhong, Y., Notaro, M., & Vavrus, S. J. (2019). Spatially variable warming of the
557 Laurentian Great Lakes: an interaction of bathymetry and climate. *Climate*
558 *Dynamics*, 52(9-10), 5833–5848. doi: 10.1007/s00382-018-4481-z
- 559
560

Supporting information for “Global heat uptake by inland waters”

I. Vanderkelen¹, N. P. M. van Lipzig², D. M. Lawrence³, B. Droppers⁴, M.

Golub⁵, S. N. Gosling⁶, A. B. G. Janssen⁴, R. Marcé^{7,8}, H. Müller

Schmied^{9,10}, M. Perroud¹¹, D. Pierson⁵, Y. Pokhrel¹², Y. Satoh¹³, J.

Schewe¹⁴, Sonia I. Seneviratne¹⁵, V. M. Stepanenko^{16,17}, R. I. Woolway¹⁸ and

W. Thiery^{1,15}

¹Vrije Universiteit Brussel, Department of Hydrology and Hydraulic Engineering, Brussels, Belgium

²KU Leuven, Department of Earth and Environmental Sciences, Leuven, Belgium

³National Center for Atmospheric Research, Boulder, Colorado, USA

⁴Wageningen University & Research, Water Systems and Global Change group, Wageningen, The Netherlands

⁵Uppsala University, Department of Ecology and Genetics, Uppsala, Sweden

⁶University of Nottingham, School of Geography, Nottingham, United Kingdom

⁷Catalan Institute for Water Research, Girona, Spain

⁸University of Girona, Girona, Spain

⁹Goethe University Frankfurt, Institute of Physical Geography, Frankfurt am Main, Germany

¹⁰Senckenberg Leibniz Biodiversity and Climate Research Centre (SBIK-F), Frankfurt am Main, Germany

¹¹University of Geneva, Institute for Environmental Sciences, Geneva, Switzerland

¹²Michigan State University, Department of Civil and Environmental Engineering, East Lansing, MI, United States

¹³National Institute for Environmental Studies, Center for Global Environmental Research, Tsukuba, Japan

¹⁴Potsdam Institute for Climate Impact Research, Transformation Pathways, Potsdam, Germany

¹⁵ETH Zurich, Institute for Atmospheric and Climate Science, Zurich, Switzerland

March 11, 2020, 8:58am

¹⁶Moscow State University, Research Computing Center, Moscow, Russia

¹⁷Moscow State University, Faculty of Geography, Moscow, Russia

¹⁸Dundalk Institute of Technology, Centre for Freshwater and Environmental Studies, Dundalk, Ireland

Contents of this file

1. Table S1
2. Figures S1 to S3

Introduction

This supplementary file contains 1 table and 3 figures providing extra information on the data and model results. Table T1 shows the used models from the Inter-sectoral Impact Model Intercomparison Project phase 2b (ISIMIP2b). Figure S1 shows maps of the input data used in the study: the area fraction for natural lakes (a), reservoirs (b) and the lake depth (c). Figure S2 illustrate the annual heat uptake by natural lakes for every individual simulation used in the analysis (per lake model and GCM forcing). Finally, figure S3 shows the terms used in the river heat uptake calculation and the resulting river heat uptake, all for both hydrological models and every GCM forcing.

Table S1. Overview of ISIMIP2b impact models used in this study.

Lake models	# layers	Lake depth	Reference
CLM4.5	10	Constant at 50 m	Subin, Riley, and Mironov (2012)
SIMSTRAT-UoG	1 - 13	GLDB	Goudsmit, Burchard, Peeters, and Wüest (2002)
Hydrological models	Human influences		Reference
MATSIRO	No human influences		Pokhrel et al. (2015)
WaterGAP2	Historical human influences		Müller Schmied et al. (2016)

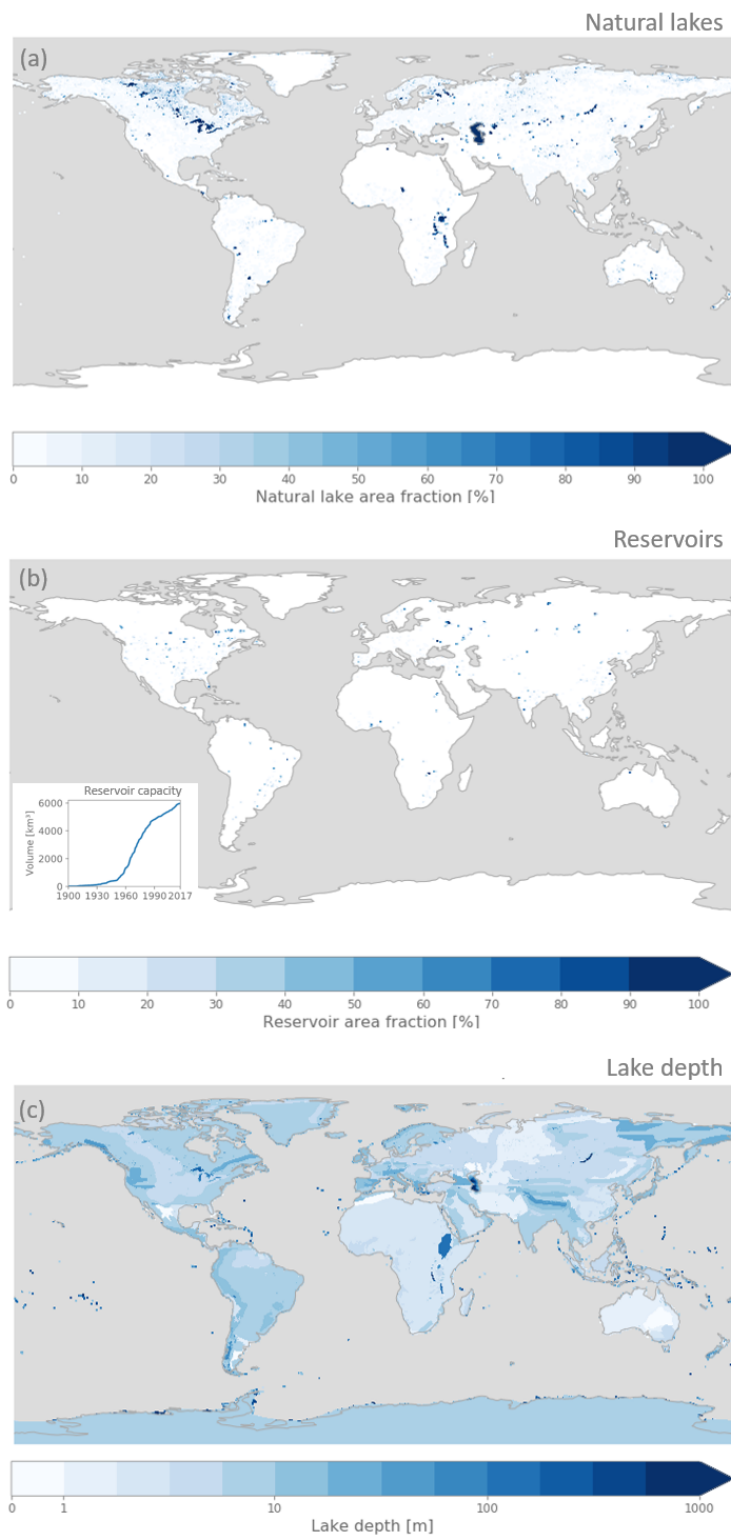


Figure S1. Lake data used in the lake heat assessment: lake area fraction, based on HydroLAKES (a; Messenger et al., 2016), reservoir area fraction map representing the reservoir expansion in the period 1900-2017, based on GRanD coupled with HydroLAKES, March 11, 2020, 8:58am inset: reservoir volume increase over time based on GRanD (b; Lehner et al., 2011; Messenger et al., 2016) and (potential) lake depth adapted from GLDB v3 (c; Choulga et al., 2019).

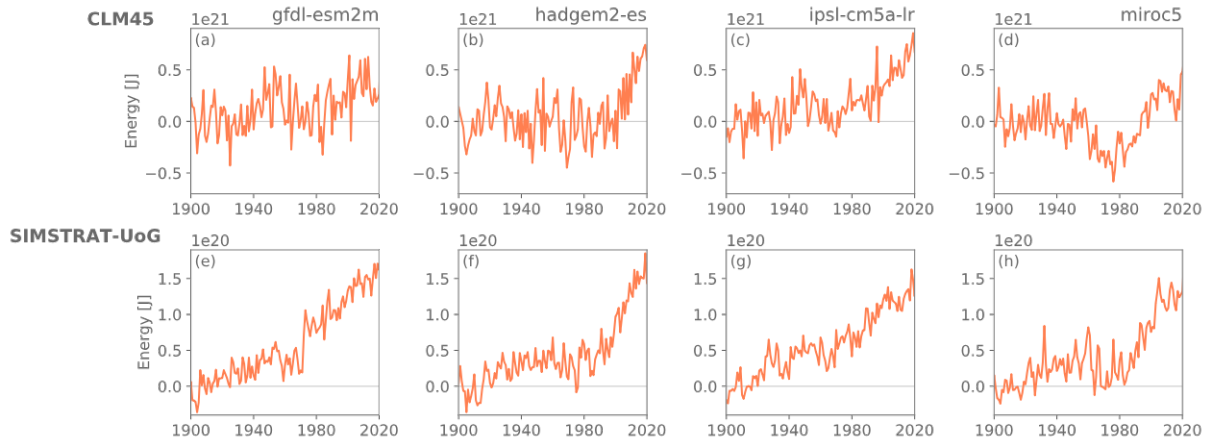


Figure S2. Annual heat uptake by natural lakes for the two different lake models (CLM45; a-d and SIMSTRAT-UoG; e-h) and ESM forcings (GFDL-ESM2M, HadGEM2-ES, IPSL-CM5A-LR, MIROC5; columns). Note the different y-axis scales.

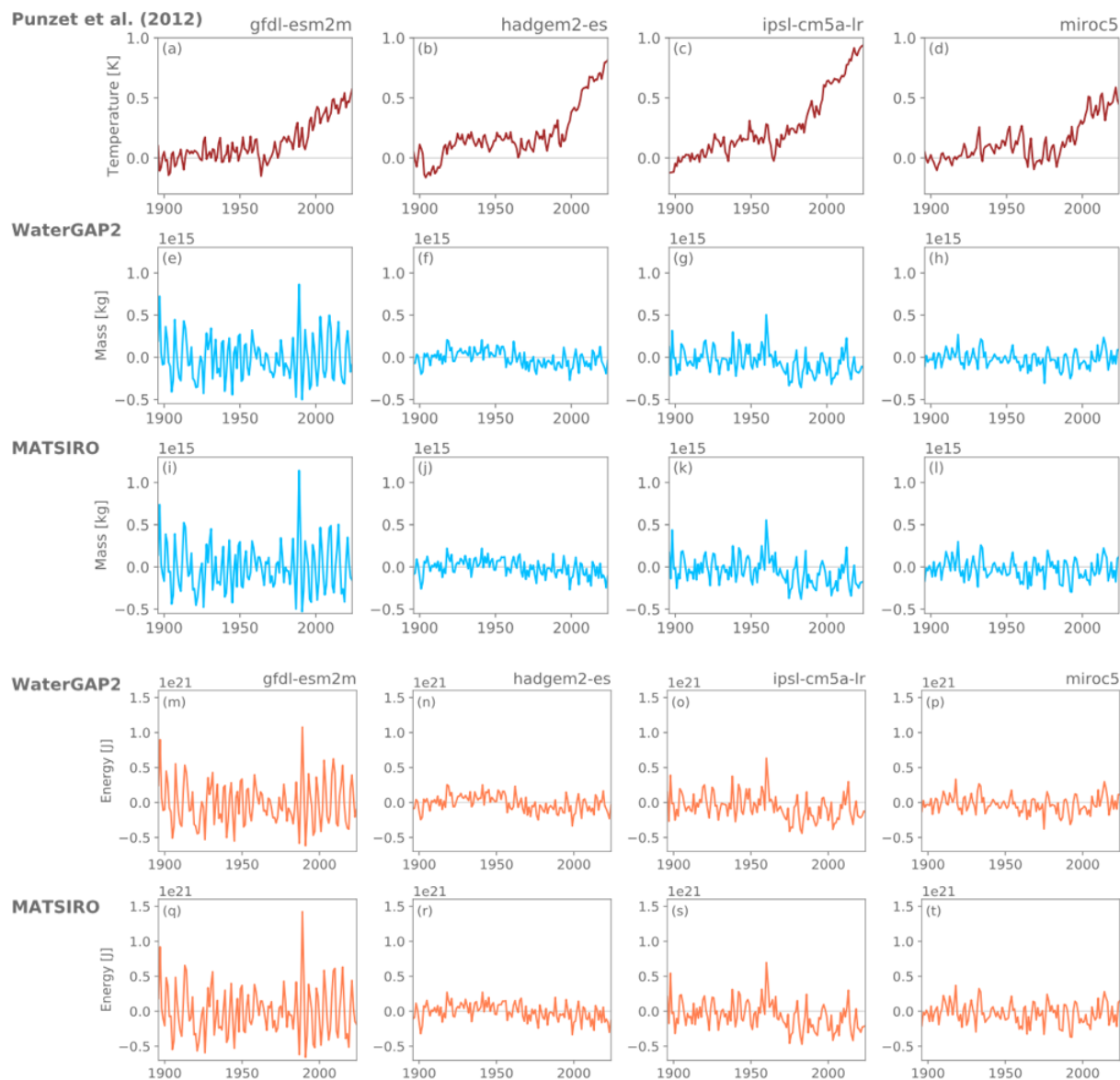


Figure S3. Global average river temperatures calculated with the parametrisation of (Punzet et al., 2012, ;a-d), global total river mass from WaterGAP2 (e-h) from MATSIRO (i-l) and resulting global river heat for WaterGAP2 (m-p) and MATSIRO (q-t), all per ESM forcing.

References

- Choulga, M., Kourzeneva, E., Balsamo, G., Boussetta, S., & Wedi, N. (2019). Upgraded global mapping information for earth system modelling: An application to surface water depth at the ECMWF. *Hydrology and Earth System Sciences*, *23*(10), 4051–4076. doi: 10.5194/hess-23-4051-2019
- Goudsmit, G. H., Burchard, H., Peeters, F., & Wüest, A. (2002). Application of k- ϵ turbulence models to enclosed basins: The role of internal seiches. *Journal of Geophysical Research C: Oceans*, *107*(12), 23–1. doi: 10.1029/2001jc000954
- Lehner, B., Liermann, C. R., Revenga, C., Vörösmarty, C., Fekete, B., Crouzet, P., ... Wisser, D. (2011). High-resolution mapping of the world's reservoirs and dams for sustainable river-flow management. *Frontiers in Ecology and the Environment*, *9*(9), 494–502. doi: 10.1890/100125
- Messenger, M. L., Lehner, B., Grill, G., Nedeva, I., & Schmitt, O. (2016). Estimating the volume and age of water stored in global lakes using a geo-statistical approach. *Nature Communications*, *7*. doi: 10.1038/ncomms13603
- Müller Schmied, H., Adam, L., Eisner, S., Fink, G., Florke, M., Kim, H., ... Doll, P. (2016). Variations of global and continental water balance components as impacted by climate forcing uncertainty and human water use. *Hydrology and Earth System Sciences*, *20*(7), 2877–2898. doi: 10.5194/hess-20-2877-2016
- Pokhrel, N. Y., Koirala, S., Yeh, P. J.-F., Hanasaki, N., Longuevigne, L., Kanae, S., & Oki, T. (2015). Incorporation of groundwater pumping in a global Land Surface Model with the representation of human impacts. *Water Resources Research*, *51*, 78–96. doi:

10.1002/2014WR015602

Punzet, M., Voß, F., Voß, A., Kynast, E., & Bärlund, I. (2012). A global approach to assess the potential impact of climate change on stream water temperatures and related in-stream first-order decay rates. *Journal of Hydrometeorology*, *13*(3), 1052–1065. doi: 10.1175/JHM-D-11-0138.1

Subin, Z. M., Riley, W. J., & Mironov, D. (2012). An improved lake model for climate simulations: Model structure, evaluation, and sensitivity analyses in CESM1. *Journal of Advances in Modeling Earth Systems*, *4*(2), 1–27. doi: 10.1029/2011MS000072